

Superconductivity and magnetism on flux grown single crystals of NiBi₃

B. Silva,¹ R.F. Luccas,¹ N.M. Nemes,² J. Hanco,¹ M.R. Osorio,¹ P. Kulkarni,¹ F. Mompean,^{3,4} M. García-Hernández,^{3,4} M.A. Ramos,^{1,4} S. Vieira,^{1,4} and H. Suderow^{*1,4}

¹*Laboratorio de Bajas Temperaturas, Departamento de Física de la Materia Condensada, Instituto Nicolás Cabrera and Condensed Matter Physics Center, Universidad Autónoma de Madrid, E-28049 Madrid, Spain*

²*Departamento de Física Aplicada III, GFMC, Universidad Complutense de Madrid, E-28040 Madrid, Spain*

³*Instituto de Ciencia de Materiales de Madrid, Consejo Superior de Investigaciones Científicas (ICMM-CSIC), Sor Juana Inés de la Cruz 3, 28049 Madrid, Spain.*

⁴*Unidad Asociada de Bajas Temperaturas y Altos Campos Magnéticos, UAM/CSIC, Cantoblanco, E-28049 Madrid, Spain*

(Dated: April 25, 2022)

We present resistivity, magnetization and specific heat measurements on flux grown single crystals of NiBi₃. We find typical behavior of a type-II superconductor, with, however, a sizable magnetic signal in the superconducting phase. There is a hysteretic magnetization characteristic of a ferromagnetic compound. By following the magnetization as a function of temperature, we find a drop at temperatures corresponding to the Curie temperature of ferromagnetic amorphous Ni. Thus, we assign the magnetism in NiBi₃ crystals to amorphous Ni impurities.

PACS numbers: 74.70.Ad,74.62.Bf,74.25.Dw

INTRODUCTION

The interplay between superconductivity and ferromagnetism has been one of the most fruitful areas of debate during recent years [1–4]. The superconducting state is generally considered to be sensitive to small concentrations of magnetic impurities, which induce Cooper pair-breaking [5–8]. But in some cases, long-range magnetic order may coexist with superconductivity [9, 10]. This leads to rather unique effects arising from the interplay between the two phenomena. Successive transitions between superconductivity and other ordered states are observed in Chevrel phase and borocarbide compounds [11–18]. Superconducting properties have been shown to be enhanced by an external field [19–23]. In heavy fermions and in hybrid proximity ferromagnetic-superconducting structures, magnetism can induce unconventional p-wave or other forms of complex superconductivity [24–28].

NiBi₃ is an intermetallic alloy known to be a type-II superconductor [29] with a critical temperature of about 4 K. Normally, Ni tends to lose its magnetic moment within this type of compounds [29]. However, recent work shows coexistence of ferromagnetic-like signals with superconductivity in polycrystalline samples [30]. Further work shows that ferromagnetism is absent in bulk single crystal samples below 300 K, but that some kind of fluctuations do exist below 150 K just at the surface [31]. In the same spirit, other authors remark the absence of ferromagnetic behavior in bulk single crystals, but show ferromagnetic and superconducting features in nanostructures. They highlight confinement effects which eventually modify the electronic band structure [32]. One of the main concerns when fabricating this kind of samples is that pure Ni in-

clusions can remain within the crystal, thus yielding a non-zero magnetic moment.

In this work, we have studied the superconducting properties of high quality NiBi₃ single crystals grown by the flux growth method. We have carried out resistivity, magnetization and specific heat measurements, with the aim to understand the magnetic and superconducting behavior of this system. We indeed find a ferromagnetic signal, also in the superconducting phase, and discuss temperature dependence of magnetization, resistivity and specific heat.

EXPERIMENTAL DETAILS

The sample was grown in excess of Bi flux [33–35]. 90% high purity Bi (Alfa Aesar 99.99%) and 10% of Ni (Alfa Aesar 99.99%) were introduced in an ampoule of quartz and sealed under inert gas atmosphere. Ampoules were heated for 4 hours until 1100°C, maintained 100 hours at this temperature, and then cooled to 300°C in 300 hours, where it remained for another 100 hours. Ampoules were then taken out of the furnace and rapidly centrifuged to remove the Bi flux. We obtained small needles of 0.1 mm×0.1 mm×1.5 mm as shown in Fig. 1. Most of these needles were joined together with residual Bi flux left over after centrifuging. We made powder X-ray diffraction on an arrangement of needles milled down to powder. We used an X’Pert PRO Theta/2Theta diffractometer with primary monochromator and fast X’Celerator detector. We measured the resistivity making four contacts on a single needle. Specific heat was determined in PPMS system of Quantum Design. To ensure proper thermalization of the whole sample, a large amount of needles (6.2 mg) were crushed down into a pellet using a force

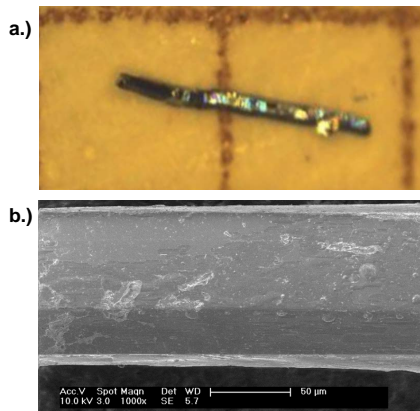


FIG. 1: a.) NiBi_3 needle of ≈ 1.2 mm length on a millimeter paper. The needle was separated mechanically from a bunch of NiBi_3 needles joined together by Bi flux. b.) Scanning Electron Microscope (SEM) picture of one needle with a cross-section of $0.1 \text{ mm} \times 0.1 \text{ mm}$. Some Bi flux bubbles can be identified.

of 5.5 tons during 6 minutes. We made magnetization hysteresis loops, $M(H)$, at constant temperature below and above T_c with a SQUID-magnetometer (MPMS) using single needles aligned parallel to the applied magnetic field.

RESULTS AND DISCUSSION

NiBi_3 has an orthorhombic CaLiSi_2 -type crystal structure with space group $pnma$. X-ray powder diffractograms are shown in Fig. 2. We find single crystalline NiBi_3 . The diffractogram also shows a peak from Bi flux used during growth (bubbles in Fig. 1b). No indication for presence of residual Ni was found in X-ray scattering. Using Rietveld refinement (X'PERT HighScore Plus software), the unit cell parameters were found to be: $a = 8.884 \text{ \AA}$, $b = 4.097 \text{ \AA}$ and $c = 11.490 \text{ \AA}$. The inset in Fig. 2 shows the NiBi_3 crystal structure[36].

The resistance strongly drops when decreasing temperature, and gives a residual resistance ratio between 4 K and 300 K of 15.3 (Fig. 3), indicating good quality single crystal. The superconducting transition starts at 4.0 K with an abrupt drop of the resistivity and ends at 3.9 K, where it becomes zero. Previous resistance and susceptibility measurements give similar residual resistivity values in single crystals[29]. Critical temperature of polycrystals and in nanostructured samples is also similar[30–32, 37].

The specific heat (Fig. 4) shows a small peak at the transition, of size expected for a weak coupling BCS superconductor, $\Delta C/T_c = 1.43\gamma$ if we take $\gamma \approx 9 \text{ mJ/K}^2\text{mol}$, which is compatible to the estimated zero

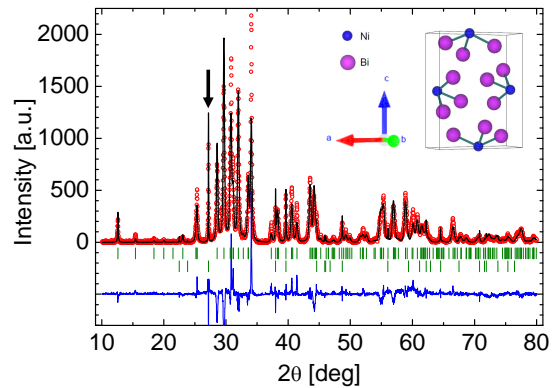


FIG. 2: X-ray powder diffraction of NiBi_3 needles. Arrows give the peaks associated to NiBi_3 . Bi flux is also identified by an arrow. In the inset we show the crystal structure of NiBi_3 .

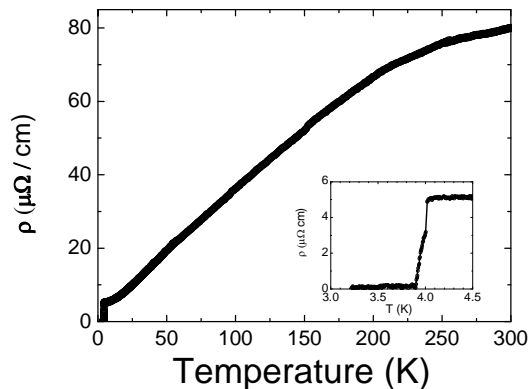


FIG. 3: In the main figure we show the temperature dependence of the resistivity between 300 K and 3.5 K. In the lower right inset we zoom into the superconducting transition at the critical temperature.

temperature extrapolation of C/T . The transition is sharp and located at the same temperature as the resistive transition. We find a small anomaly around 2.2 K, which depends of applied magnetic field. The contribution to the specific heat from this anomaly extends to temperatures well above the position of the kink. Actually, in a conventional BCS superconductor, the zero field specific heat should fall below the normal state specific heat approximately around $0.6 T_c$. Here, the zero field specific heat remains above the 5 T specific heat over the whole temperature range. The observed anomaly at 2.2 K is of magnetic origin and of same order than electronic and phonon contributions. A magnetic transition at this temperature involving the whole sample should give an

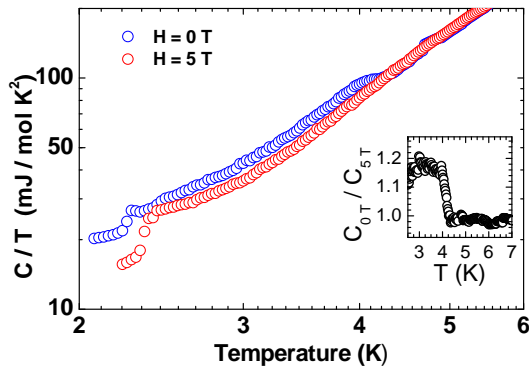


FIG. 4: Specific heat divided by temperature C/T as a function of temperature T for NiBi_3 at zero magnetic field (red points) and at 5 T (blue points). Inset shows the jump at the superconducting transition as the zero field divided by the high magnetic field specific heat around T_c .

overwhelming contribution to the specific heat [34, 38]. Therefore, this anomaly is not due to a full bulk magnetic transition but rather to residual magnetism. No traces of this transition are found in other measurements. The specific heat measurements are the only ones made using pressed powder and not single crystals. Probably, the procedure of crushing the needles into a pellet has brought about a magnetic transition in a small part of the crushed pellet.

The main panel of Fig. 5 shows the magnetization of NiBi_3 single crystal at 1.8 K. The solid curve corresponds to the first increase of the field after zero field cooling (ZFC) and the dashed line to a decreasing field. From the minimum in the transition between Meissner and Shubnikov states we find $\mu_0 H_{c1} = 12$ mT. The normal state is reached at $\mu_0 H_{c2} = 0.35$ T indicated by a change in the slope of $M(H)$. The magnetization curves within the superconducting state are rather closed, and we find a reversible behavior over a significant range of magnetic fields. This is expected in a high purity single crystalline sample with low pinning. Single crystalline samples grown by the solid state method give small hysteresis loops [30], similar to ours. Other samples grown by encapsulation of stoichiometric powder, which show grains and some inhomogeneities, also present larger hysteresis loops [37]. The magnetization loops with highest hysteresis were for samples grown by a reductive etching of $\text{Bi}_{12}\text{Ni}_4\text{I}_3$ [32].

From $\frac{H_{c2}(0)}{H_{c1}(0)} = \frac{2\kappa^2}{\ln(\kappa)}$, (where $H_{c1,2}(0)$ are zero temperature extrapolations of first and second critical fields), $H_{c2}(0) = \frac{\phi_0}{2\pi\mu_0\xi^2}$ and $\kappa = \frac{\lambda}{\xi}$, we find $\kappa = 5.29 \pm 0.01$, $\xi = 300 \pm 10$ Å and $\lambda = 1600 \pm 200$ Å. The thermodynamic critical magnetic field is $H_c(0) = 50 \pm 3$ mT (from

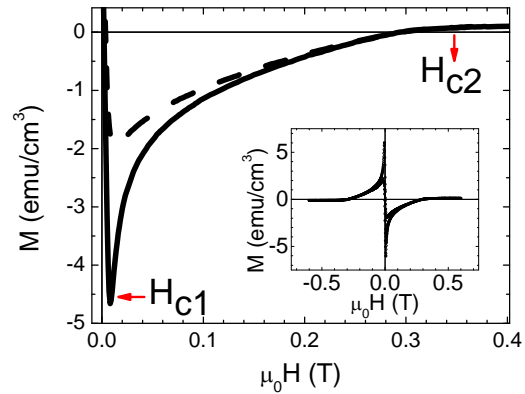


FIG. 5: Magnetization as a function of magnetic field at 1.8 K. The continuous line shows increasing field after ZFC. The dashed line shows decreasing field from 6 T. Arrows indicate the superconducting critical fields. Inset shows the full magnetization loop.

$$H_{c1}(0) = \frac{H_c(0)}{\sqrt{2\kappa}} \ln(\kappa).$$

At magnetic fields above H_{c2} , the magnetization shows a peculiar behavior, characterized by a finite magnetization, typical of a ferromagnet.

When we increase the temperature above T_c , we can remove the superconducting signal and find the ferromagnetic behavior. It gives hysteresis loops as shown in Fig. 6. The saturation field is small, but well defined ($M_S = 0.013$ emu/g). The loops are rather closed, with a coercitive field of 2.0 mT, and remanence of $M_r = 0.0008$ emu/g (inset of Fig. 6). The saturation magnetization corresponds to $\approx 1.74 \cdot 10^{-3} \mu_B/\text{Ni}$ as compared to the $M_S \approx 0.616 \mu_B/\text{Ni}$ of elemental ferromagnetic Ni. Thus, magnetism is residual. These values do not change when entering the superconducting phase.

Curves in Fig. 5 have been taken after room temperature demagnetizing the ferromagnetic signal. However, if we do not demagnetize, we observe flux trapping in the superconductor by the remanent field. The magnetization curves remain similar as in Fig. 5, without additional irreversibility. Thus, the ferromagnetic signal does not produce a strong pinning effect. This is compatible with the soft magnetic features and reminds the situation found in permalloy-superconductor nanostructures [39].

We measured the magnetization of the NiBi_3 crystals up to 700 K to search for eventual high-temperature disappearance of the ferromagnetic signal (Fig. 7). We find indeed a jump and change of slope at $T = 525$ K with no further transition until 700 K. The Curie temperature of crystalline Ni is at $T_C = 631$ K. Thus, the magnetic component is not due to crystalline Ni inclusions. The lack of peaks in X-ray scattering from crystalline Ni implies that there are no crystallized Ni impurities larger than the X-

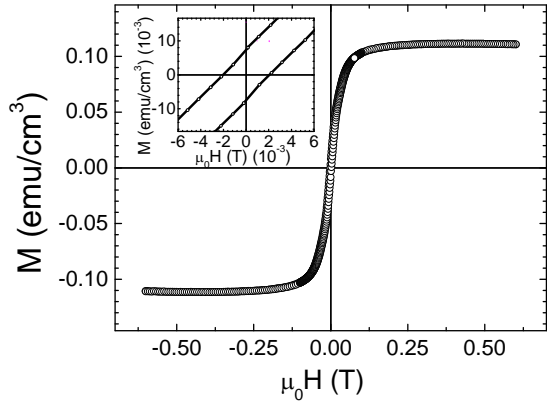


FIG. 6: Magnetization hysteresis loop at 10 K. The inset gives a zoom to highlight the behavior close to zero field. Note that the hysteresis is small, indicating soft ferromagnetism.

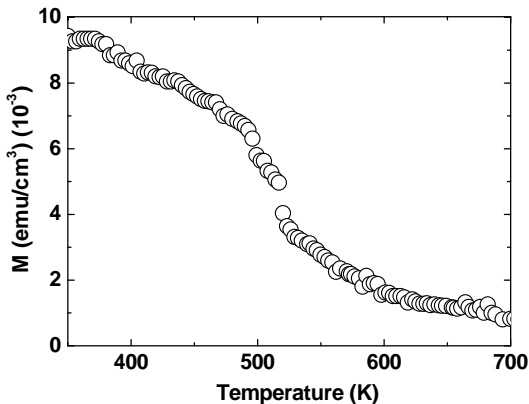


FIG. 7: Magnetization of NiBi₃ at high temperatures, in an applied magnetic field of 1 mT. Note the transition at 525 K, close to the Curie temperature of amorphous Ni.

ray coherence length of a few 100 Å. This, of course, does not exclude amorphous Ni. Amorphous Ni is a ferromagnet with a Curie temperature $T_C = 530$ K. This value is very close to the observed change of slope of Fig. 7 [40]. We thus conclude that amorphous Ni inclusions produce the observed coexistence of superconductivity and magnetism in this system.

SUMMARY AND CONCLUSIONS

We have prepared NiBi₃ single crystal with the flux-growth method, which shows good type II superconducting behavior along with ferromagnetism. We have measured resistivity, specific heat and magnetization. Resistivity shows that we have prepared good quality single

crystalline samples, and from specific heat, we obtain a full superconducting transition. In the magnetization curves we find, at the same time, superconducting and ferromagnetic signals. We have shown that the ferromagnetic signal seen in the magnetization experiments stems from amorphous Ni inclusions in the superconducting NiBi₃ matrix. Thus, the coexistence of ferromagnetism and superconductivity in this system is extrinsic.

This intermetallic system is prone to give, at the local scale, interesting situations where magnetism and superconductivity show some interplay. This may lead to anomalous proximity effects or vortex pinning features [24, 41]. Nanofabrication in form of wires or other structures [32] could make use of the likely formation of magnetic inclusions by controlling their position and size.

ACKNOWLEDGEMENTS

This work was supported by the Spanish MINECO (FIS2011-23488, ACI-2009-0905 and MAT2011-27470-C02-02), by the Comunidad de Madrid through program Nanobiomagnet. We acknowledge P.C. Canfield for teaching us the flux growth method. We also acknowledge Banco Santander for support in setting up the flux growth bench and COST 1201 action.

* Corresponding author: hermann.suderow@uam.es.

-
- [1] P. C. Canfield, P. L. Gammel, and D. J. Bishop, *Physics Today* **51**, 40 (1998).
 - [2] S. A. Kivelson, G. Aeppli, and V. J. Emery, *Proc. Nat. Acad. Sci.* **98**, 11903 (2001).
 - [3] D. Aoki, A. Huxley, E. Ressouche, D. Braithwaite, J. Flouquet, J.-P. Brison, E. Lhotel, and C. Paulsen, *Nature* **413**, 613 (2001).
 - [4] E. Coronado, C. Marti-Gastaldo, E. Navarro-Moratalla, A. Ribera, S. Blundell, and P. Baker, *Nat. Chem.* **2**, 1031 (2010).
 - [5] B. T. Matthias, *Phys. Rev.* **92**, 874 (1953).
 - [6] J. A. Chervenak and J. M. Valles, *Phys. Rev. B* **51**, 11977 (1995).
 - [7] D. Garrett, H. Beckmann, and G. Bergmann, *Phys. Rev. B* **57**, 2732 (1998).
 - [8] R. A. Smith and V. Ambegaokar, *Phys. Rev. B* **62**, 5913 (2000).
 - [9] J. Flouquet and A. Buzdin, *Physics World* **15**, 41 (2002).
 - [10] L. N. Bulaevskii, A. I. Buzdin, M. L. Kulić, and S. V. Panjukov, *Advances in Physics* **34**, 175 (1985).
 - [11] W. A. Fertig, D. C. Johnston, L. E. DeLong, R. W. McCallum, M. B. Maple, and B. T. Matthias, *Phys. Rev. Lett.* **38**, 987 (1977).
 - [12] H. R. Ott, W. A. Fertig, D. C. Johnston, M. B. Maple, and B. T. Matthias, *J. Low Temp. Phys.* **33**, 159 (1978).
 - [13] J. W. Lynn, J. A. Gotaas, R. N. Shelton, H. E. Horng, and C. J. Glinka, *Phys. Rev. B* **31**, 5756 (1985).
 - [14] R. Prozorov, M. D. Vannette, S. A. Law, S. L. Bud'ko, and P. C. Canfield, *Phys. Rev. B* **77**, 100503 (2008).

- [15] V. Crespo, J. G. Rodrigo, H. Suderow, S. Vieira, D. G. Hinks, and I. K. Schuller, *Phys. Rev. Lett.* **102**, 237002 (2009).
- [16] M. Crespo, H. Suderow, S. Vieira, S. Bud'ko, and P. C. Canfield, *Phys. Rev. Lett.* **96**, 027003 (2006).
- [17] J. Galvis, M. Crespo, I. Guillamón, H. Suderow, S. Vieira, M. G. Hernández, S. Bud'ko, and P. Canfield, *Solid State Communications* **152**, 1076 (2012).
- [18] M. Crespo, H. Suderow, S. Vieira, S. Bud'ko, and P. C. Canfield, *Physica B: Condensed Matter* **378-80**, 471 (2006).
- [19] M. B. Maple, *Physics Today* **39**, 72 (1986).
- [20] S. Sangiao, J. M. De Teresa, M. R. Ibarra, I. Guillamón, H. Suderow, S. Vieira, and L. Morellón, *Phys. Rev. B* **84**, 233402 (2011).
- [21] I. Guillamon, M. Crespo, H. Suderow, S. Vieira, J. P. Brison, S. L. Bud'ko, and P. C. Canfield, *Physica C* **470**, 771 (2010).
- [22] H. Suderow, P. Martinez-Samper, N. Luchier, J. P. Brison, S. Vieira, and P. C. Canfield, *Phys. Rev. B* **64**, 020503 (2001).
- [23] R. Cordoba and et al., *Nat. Comm.* **4**, 1437 (2013).
- [24] A. I. Buzdin, *Rev. Mod. Phys.* **77**, 935 (2005).
- [25] F. Steglich, J. Aarts, C. D. Bredl, W. Lieke, D. Meschede, W. Franz, and H. Schäfer, *Phys. Rev. Lett.* **43**, 1892 (1979).
- [26] J.-P. Brison, L. Glémot, H. Suderow, A. Huxley, S. Kambe, and J. Flouquet, *Phys. B* **280**, 165 (2000).
- [27] F. Steglich, *Phys. B* **359-61**, 326 (2005).
- [28] F. Steglich, O. Stockert, S. Wirth, C. Geibel, H. Q. Yuan, S. Kirchner, and Q. Si, arXiv:1208.3684 (2012).
- [29] Y. Fujimori, S. Kan, B. Shinozaki, and T. Kawaguti, *J. Phys. Soc. Jpn.* **69**, 3017 (2000).
- [30] E. L. Martinez Piñeiro, B. L. Ruiz Herrera, R. Escudero, and L. Bucio, *Solid State Commun.* **151**, 425 (2011).
- [31] X. Zhu, H. Lei, C. Petrovic, and Y. Zhang, *Phys. Rev. B* **86**, 024527 (2012).
- [32] T. Herrmannsdörfer, R. Skrotzki, J. Wosnitzer, D. Köhler, R. Boldt, and M. Ruck, *Phys. Rev. B* **83**, 140501 (2011).
- [33] P. C. Canfield and Z. Fisk, *Phil. Mag. B* **65**, 1117 (1992).
- [34] P. C. Canfield, B. K. Cho, and K. W. Dennis, *Physica B* **215**, 337 (1995).
- [35] P. C. Canfield, *Solution growth of intermetallic single crystals: a beginner's guide.* (2009), chap. 2, pp. 93–111.
- [36] M. Ruck and T. Z. Söhnle, *Z. Naturforsch. B: Chem. Sci.* **61**, 785 (2006).
- [37] J. Kumar, A. Kumar, A. Vajpayee, B. Gahtori, D. Sharma, P. K. Ahluwalia, S. Auluck, and V. P. S. Awana., *Supercond. Sci. Technol* **24**, 085002 (2011).
- [38] L. Durivault and et al., *J. Phys. Cond. Matt.* **15**, 77 (2003).
- [39] Z. Yang, M. Lange, A. Volodin, R. Szymczak, and V. Moshchalkov, *Nature Mater.* **3**, 793 (2004).
- [40] K. Tamura and H. Endo, *Phys. Lett. A* **29**, 52 (1969).
- [41] G. Blatter, M. V. Feigel'man, V. B. Geshkenbein, A. I. Larkin, and V. M. Vinokur, *Rev. Mod. Phys.* **66**, 1125 (1994).